

Molecular Dynamics of *n*-Octane Inside Zeolite ZSM-5 As Studied by Deuterium Solid-State NMR and Quasi-Elastic Neutron Scattering

Alexander G. Stepanov, Alexander A. Shubin, and Mikhail V. Luzgin

*Boriskov Institute of Catalysis, Siberian Branch of the Russian Academy of Sciences,
Prospekt Akademika Lavrentieva 5, Novosibirsk 630090, Russia*

Hervé Jobic* and Alain Tuel

Institut de Recherches sur la Catalyse, CNRS, 2 av. Albert Einstein, 69626 Villeurbanne, France

Received: June 26, 1998; In Final Form: September 23, 1998

The dynamics of a linear alkane, *n*-octane, adsorbed in zeolite ZSM-5 was studied using deuterium solid-state NMR (^2H NMR) and quasi-elastic neutron scattering (QENS). It has been found that at the loading of 1.8 molecules per unit cell, adsorbed *n*-octane molecules are essentially located in the straight channels and diffuse along the direction of the straight channels with a diffusion coefficient $D = 12.0 \times 10^{-11} \text{ m}^2/\text{s}$ at 300 K. In the course of translational movement along the straight channels, some coupled rotational motions of all CH_n ($n = 2, 3$) groups of the hydrocarbon skeleton of the molecule take place. They are reflected in the ^2H NMR spectrum of deuterated *n*-octane- d_{18} , in the temperature range 253–373 K, as fast rotations of the separate methylene and methyl groups simultaneously around two and three C–C bonds of the molecule with a characteristic time $\tau_C \approx 10^{-11} \text{ s}$ and an activation energy $E_R \approx 10\text{--}12 \text{ kJ/mol}$. These internal motions may correspond to fast interconversion between trans and gauche conformations in the adsorbed alkane molecule while the molecule moves along the straight channels. Upon heating at 373 K for 1 h, *n*-octane molecules, formerly located in the straight channels, become redistributed over straight and zigzag channels. Subsequent translational motion of *n*-octane consists of two independent modes of motion. One of them represents the movement along the tortuous zigzag channels. The other one represents the movement along the straight channels, disturbed by collisions with the other molecules at the channel intersections. For a loading of 3.5 molecules per unit cell, a liquidlike line shape appears at 253 K in the ^2H NMR spectrum. This line shape corresponds to isotropically reorienting *n*-octane molecules, changing the direction of their translational motion (from straight to zigzag channels) under collision with the other molecules at the channel intersections.

Introduction

Study of the dynamic behavior of alkanes sorbed by zeolites is of crucial importance for practical catalysis and of interest from a theoretical point of view. A number of important industrial processes, which involve alkanes, use zeolites either as catalysts or sorbents, e.g., in fluid catalytic cracking¹ or for hydrocarbon separation.² Diffusion of hydrocarbon molecules inside zeolite pores plays a critical role in the performances of zeolitic materials as catalysts and adsorbents. Therefore, it is no wonder that much work has been done to measure and characterize the diffusion of hydrocarbons in zeolites.^{3,4} From the theoretical point of view, it is of particular interest to have a knowledge of the dynamic properties of long-chain hydrocarbon molecules whose dimensions are commensurable with the sizes of zeolitic pores. The information on the dynamic behavior of large molecules in constrained geometries, whose dynamics are strongly affected by both the zeolitic walls and the regular periodicity of the zeolitic pore system, should aid in elucidating the origin of shape selectivity⁵ in catalytic reactions and may be the basis for the development of models for large molecule diffusion and for clarifying the mechanism of diffusion.

The mobilities of hydrocarbons sorbed within zeolites are usually probed with pulsed-field gradient NMR (PFG NMR)

or quasi-elastic neutron scattering (QENS) techniques.^{6,7} These techniques yield information on the intracrystalline diffusion coefficients. By using neutron spectrometers with different time scales, the QENS method can be used to characterize rotational motions.^{8,9} This information can also be derived from the analysis of deuterium solid-state NMR (^2H NMR) spectra of adsorbed deuterated molecules.^{10–16} The line shape for ^2H NMR is defined completely by intramolecular quadrupole interaction.^{17–19} An important point is that the line shape of the ^2H NMR spectrum is especially sensitive to the mode of molecular motion and its rate.^{18,19} Therefore, by analyzing ^2H NMR line shapes as well as relaxation rates, one can evaluate the nature of the molecular motion and its rate.

Up to now, the dynamics of long-chain linear alkanes ($\text{C}_8\text{--}\text{C}_{20}$) in silicalite, the Al-free analogue of ZSM-5, has been probed only by theoretical methods.^{20–22} However, molecular dynamics (MD) simulations of alkanes in silicalite give some idealized view of alkane motion inside the zeolite channels, which may be different from the real dynamic behavior. Therefore, for clarifying the dynamics of linear long-chain alkanes in the catalytically active ZSM-5 zeolite, experimental techniques such as ^2H NMR and QENS studies are expected to be useful.

In this paper, we report the results of ^2H NMR and QENS studies of the dynamic behavior of linear *n*-octane inside ZSM-5 zeolite. ZSM-5 was chosen for this work because of the

* To whom correspondence should be addressed. E-mail: jobic@catalyse.univ-lyon1.fr. Fax: (33) 4 72 44 53 99.

industrial importance of this zeolite²³ and because the dynamics of linear long-chain alkanes is already well-characterized by theoretical methods.^{20–22} This allows one to compare the possibilities of theoretical and experimental techniques for probing the real dynamics of adsorbed molecules inside the zeolites. The pore system of ZSM-5 contains two types of interconnected channels, which consist of 10-membered oxygen rings. Straight channels with dimensions of 5.4×5.6 Å are interconnected in the perpendicular direction by zigzag channels with dimensions 5.5×5.1 Å. These two channels meet at a relatively open intersection region, having a roughly spherical shape with a diameter of about 8 Å.²⁴

By simultaneous application of ²H NMR and QENS methods, we have succeeded in obtaining new knowledge on both the peculiarities of adsorption of *n*-octane and its motional behavior inside the specific pore system of the zeolite ZSM-5.

Experimental Section

Materials. For the ²H NMR experiments, the H-ZSM-5 sample with a Si/Al ratio of 58 was prepared from Na-ZSM-5 via NH₄⁺ ion exchange and subsequent calcination at 820 K as described in ref 25. The obtained zeolite sample was characterized by X-ray powder diffraction and chemical analyses. Perdeuterated *n*-octane-*d*₁₈ with 98% ²H isotope enrichment was used in this work. For the QENS measurements, the ZSM-5 sample (Si/Al = 36) was used under sodium form to decrease the signal due to the zeolite.

Sample Preparation. To prepare samples for the NMR experiments, approximately 0.3 g of zeolite was loaded in a 5 mm (o.d.) glass tube connected to a vacuum system. The sample was then heated at 720 K for 1.5 h in air and for 4 h under vacuum to a final pressure above the sample of 10^{-5} Torr (1 Torr = 133.3 Pa). After the sample was cooled back to room temperature, the zeolite was exposed to the vapor of previously degassed *n*-octane-*d*₁₈ (ca. 8 Torr according to a mercury manometer) in the calibrated volume (140 mL). It took a few minutes for complete consumption of *n*-octane vapor to occur. The adsorption procedure was repeated several times until the desired amount of adsorbed alkane was achieved, i.e., 200–900 μmol/g (1.8–5.3 molecules per unit cell). This step-by-step procedure for the alkane adsorption (60 μmol of *n*-octane in each step) was used to avoid potentially possible condensation of the alkane on the outer surface of the zeolite crystallites. After adsorption, the neck of the tube was sealed off while the zeolite sample was maintained in liquid nitrogen in order to prevent its heating by the flame. The sealed sample was then transferred into an NMR probe for recording the ²H NMR spectra.

For the QENS experiments, 3 g of zeolite was activated by heating to 770 K under flowing oxygen. The sample was cooled and pumped to 10^{-4} Pa while heating again to 770 K. After cooling, *n*-octane was adsorbed onto the pretreated zeolite (loading: 2 molecules per unit cell). The sample was transferred inside a glovebox into a cylindrical aluminum container of annular geometry. A similar cell containing the same amount of dehydrated ZSM-5 was also prepared.

NMR Measurements. ²H NMR experiments were performed at 61.42 MHz on a Bruker MSL-400 spectrometer using a high-power probe with a 5 mm horizontal solenoid coil. All ²H NMR spectra were obtained by Fourier transformation of the quadrature-detected quadrupole echo arising in a pulse sequence²⁶

$$\left(\frac{\pi}{2}\right)_{\pm X} - \tau_1 - \left(\frac{\pi}{2}\right)_Y - \tau_2 - \text{acquisition} - t \quad (i)$$

where $\tau_1 = 30$ μs, $\tau_2 = 34$ μs, and t is a repetition time for the sequence (i) during the accumulation of NMR signal. The duration of the $\pi/2$ pulses was 3.0–4.0 μs. Spectra were typically obtained with 500–5000 scans and a repetition time of $t = 0.4$ –2 s. Inversion–recovery experiments, to derive spin–lattice relaxation times (T_1), were carried out using the pulse sequence²⁷

$$(\pi)_X - t_v - \left(\frac{\pi}{2}\right)_{\pm X} - \tau_1 - \left(\frac{\pi}{2}\right)_Y - \tau_2 - \text{acquisition} - t \quad (ii)$$

where t_v was a variable delay between the 180° (π)_X inverting pulse (as in a standard inversion–recovery pulse sequence²⁷) and the quadrupole echo sequence (i). In the case of overlapping of different signals to the overall ²H NMR line shape, T_1 values were calculated on the basis of the time τ_0 ($\tau_0 = 0.693T_1$). τ_0 is the time for which the intensity of the NMR line turns from an inverted negative position to the normal positive one in the inversion–recovery experiment (sequence ii).

The temperature of the samples was controlled with a flow of nitrogen gas, stabilized with a variable-temperature unit BVT-1000 with a precision of about 1 K.

QENS Measurements. The neutron experiments were performed on the new backscattering spectrometer IN16 at the Institut Laue-Langevin in Grenoble. This spectrometer improves both the neutron flux and the energy resolution over existing backscattering spectrometers by applying focusing techniques. A resolution of 1 μeV was selected; this allows one to study diffusive motions on a time scale of 0.5–10 ns. With this instrument, the energy transfers are scanned by varying the incident energy by Doppler shift, keeping the final energy fixed. The energy transfer, $\hbar\omega$, is analyzed in a window of ± 12 μeV. The momentum transfer, $\hbar Q$, depends on the scattering angle; in our experiment the Q -range was 0.19–1.7 Å^{−1}.

Theoretical Background. NMR. ²H NMR spectra from polycrystalline organic solids are known to be dominated by quadrupole coupling.^{17–19,28,29} This coupling is of intramolecular origin^{17–19} and is strongly affected by the mode and rate of the molecular motion in which a molecule is involved.^{18,28–30}

For molecules that are rigid on the ²H NMR time scale, τ_{NMR} (i.e., when correlation times τ_C for molecular reorientation and internal motions satisfy the condition $\tau_C \gg \tau_{\text{NMR}} \approx Q_0^{-1} \approx 5 \times 10^{-6}$ s, where $Q_0 = C_Q = e^2 q Q / h$ is the quadrupole coupling constant unaffected by any motional averaging),³¹ ²H NMR spectra represent Pake-type powder patterns.^{18,19} The dominant features of these line shapes are two strong peaks separated by the splitting $3/4 Q_0$ and two shoulders separated by $3/2 Q_0$ (see Figure 1A). For deuterium bonded to tetrahedral carbon atoms in polycrystalline organic solids, $3/4 Q_0$ is usually 120–130 kHz and the asymmetry parameter η is close to zero.^{28,30,32} If a CD₃ group of an organic molecule undergoes fast 3-fold jumps or diffusional rotation about the C–CD₃ bond with a correlation time $\tau_R \ll \tau_{\text{NMR}}$, i.e., $\tau_R < 10^{-7}$ to 10^{-6} s and if isotropic reorientation of the molecule as a whole is slow ($\tau_C \gg \tau_{\text{NMR}}$), then the line shape of the spectrum for CD₃ groups will be similar to that of rigid molecules but with the quadrupole splitting reduced to a value of $3/4 Q_1$ (Figure 1B),^{30,32,33} according to the relation

$$Q_1 = Q_0 \frac{3 \cos^2 \alpha - 1}{2} \quad (1)$$

Here, α is the rotation angle between C–D and C–CD₃ bonds. For the ideal tetrahedral geometry of the C–CD₃ fragment, α

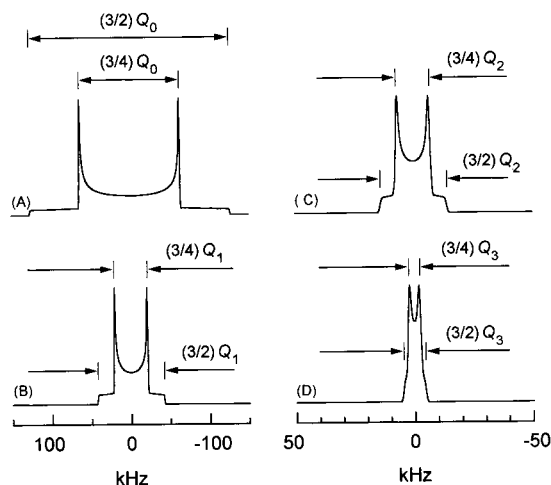


Figure 1. Theoretical ^2H NMR spectra. (A) Polycrystalline sample (static CD_3^- group, $C_Q = e^2qQ/h = Q_0 = 169.5$ kHz, $\eta = 0$); (B) Rapid rotation of the CD_3^- group about one C_3 axis, angle $\alpha = 109.47^\circ$, $Q_1 = 1/3Q_0$; (C) Rapid rotation of the CD_3^- group about two C_3 axes, angles $\alpha = \beta = 109.47^\circ$, $Q_2 = 1/9Q_0$; (D) Rapid rotation of the CD_3^- group about three C_3 axes, angle $\alpha = \beta = \gamma = 109.47^\circ$, $Q_3 = (1/27)Q_0$. An individual line shape function $g(x) = 1/\sigma\sqrt{2\pi} \exp(-x^2/2\sigma^2)$ with $\sigma = 0.5$ kHz was used in all simulations.

$= 109.47^\circ$ and $Q_1 = 1/3Q_0$. In practice, typical values of the reduced splitting $3/4Q_0$ are 35–40 kHz.^{30,33,34}

If a CD_3 group is involved in additional rotation (either three- or higher-fold jumps) about a second axis tilted at the angle β with respect to the first axis, then, again, its ^2H NMR spectrum has a quadrupole splitting reduced to $3/4Q_2$ ³⁵ (Figure 1C) with an effective quadrupole constant equal to

$$Q_2 = Q_0 \left(\frac{3 \cos^2 \alpha - 1}{2} \right) \left(\frac{3 \cos^2 \beta - 1}{2} \right) \quad (2)$$

For $\beta \approx 109.47^\circ$, this splitting is typically $3/4Q_2 \approx 12$ –14 kHz. Similarly, in the case of the existence of a third rotation (jump) axis there will be a further reduction of the quadrupole splitting up to $3/4Q_3$, where

$$Q_3 = Q_0 \left(\frac{3 \cos^2 \alpha - 1}{2} \right) \left(\frac{3 \cos^2 \beta - 1}{2} \right) \left(\frac{3 \cos^2 \gamma - 1}{2} \right) \quad (3)$$

Thus, for tetrahedral angles $\alpha = \beta = \gamma = 109.47^\circ$, the finally observed splitting is $3/4Q_3 = 1/36Q_0$.

When the correlation time τ_C for the isotropic reorientation (rotation) of the molecule as a whole becomes comparable to τ_{NMR} , a broadening of the spectrum is observed and the sharp features disappear.³¹ For rapid isotropic reorientation, as in liquids, when $\tau_C \ll \tau_{\text{NMR}}$, the quadrupole splitting is averaged to zero and a single line with a Lorentzian shape is observed at ν_L , the Larmor frequency of the deuterium nucleus (in Hertz). The width at half-height of this line is given by the equation:¹⁷

$$\Delta\nu_{1/2} = \frac{1}{\pi T_2} = \frac{3\pi}{20} Q_0^2 \left(1 + \frac{\eta^2}{3} \right) \times \left(3\tau_C + \frac{5\tau_C}{1 + \omega_I^2 \tau_C^2} + \frac{2\tau_C}{1 + 4\omega_I^2 \tau_C^2} \right) \quad (4)$$

Here $\omega_I = 2\pi\nu_I$ and $\tau_C = (6D_{\text{iso}})^{-1}$, where D_{iso} is the rotational diffusion coefficient for isotropic reorientation.

Although ^2H NMR line shape provides information about the type of motion for a CD_3 group in a molecule, it contains no

further information about the rates of this process if the anisotropic motion is fast on the ^2H NMR time scale. For a number of experimental situations, this information may be obtained from the special measurements of nuclear relaxation rates.³⁶ Under the same conditions as above, spin–lattice relaxation time T_1 for the “liquidlike” spectra is given by the following equation¹⁷

$$\frac{1}{T_1} = \frac{3}{40} \left(1 + \frac{\eta^2}{3} \right) (2\pi Q_0)^2 \left(\frac{\tau_C}{1 + \omega_I^2 \tau_C^2} + \frac{4\tau_C}{1 + 4\omega_I^2 \tau_C^2} \right) \quad (5)$$

which has a relatively simple form suitable for a semiquantitative estimation of the correlation time τ_C on the high-temperature side of the T_1 minimum, i.e., where $\tau_C \ll \omega_I^{-1}$ (extreme narrowing limit):

$$\frac{1}{T_1} = \frac{3}{8} \left(1 + \frac{\eta^2}{3} \right) (2\pi Q_0)^2 \tau_C \quad (6)$$

In fact, the exact value of the proportionality coefficient between $1/T_1$ and τ_C (as well as the definition of τ_C itself) depends on the model of the motion. For example, explicit expressions for T_1 for three-site jumps and for continuous diffusion of a CD_3 group about a symmetry axis in a static solid were developed by Torchia and Szabo.³⁶ According to their results for deuterons of a methyl group in the extreme narrowing limit and for $\eta = 0$, the spin–lattice relaxation rate ($1/T_1$) for three-site jump model is defined by the expression:

$$\frac{1}{T_1} = \frac{1}{4} (2\pi Q_0)^2 (1 + \cos^2 \theta) \tau_C \quad (7)$$

Here θ is an angle between the magnetic field and the 3-fold symmetry axis, $\tau_C = (3k)^{-1}$, and k is the rate constant for jumping between neighboring sites. Under the same conditions, for C–D bond continuous diffusion

$$\frac{1}{T_1} = \frac{1}{6} (2\pi Q_0)^2 \tau_C \quad (8)$$

where $\tau_C = D^{-1}$ and D is the diffusion coefficient about a symmetry axis.

QENS. Rotational and translational motions of molecules adsorbed in zeolites broaden the elastic peak associated with neutrons scattered without energy transfer, hence the term quasi-elastic. These unquantified diffusive motions yield a continuous spectrum in an energy domain ± 2 meV. For hydrocarbons, only incoherent scattering has to be considered because of the large incoherent cross section of hydrogen. The intensity scattered by the sample, after subtraction of the contribution from the dehydrated zeolite, is proportional to the incoherent scattering function, $S(\mathbf{Q}, \omega)$, where $\hbar\omega$ is the neutron energy transfer and $\hbar\mathbf{Q}$ the momentum transfer. This scattering function is related to self-motions of the hydrogen atoms under the effect of the different molecular motions.³⁷

In previous studies of mobilities of n -alkanes in ZSM-5,^{38–40} only the mean diffusivity (an average along the three crystallographic directions) could be derived from the QENS spectra. Reasonable values of the diffusion coefficients were obtained because the broadenings due to diffusion at small Q values (corresponding to large distances) were not large when compared with the instrumental resolution. A jump diffusion model was used to obtain additional information on the diffusion mechanism: the molecule remains on a given site (or in a region of space of deep potential) during a time τ_0 and then diffuses during

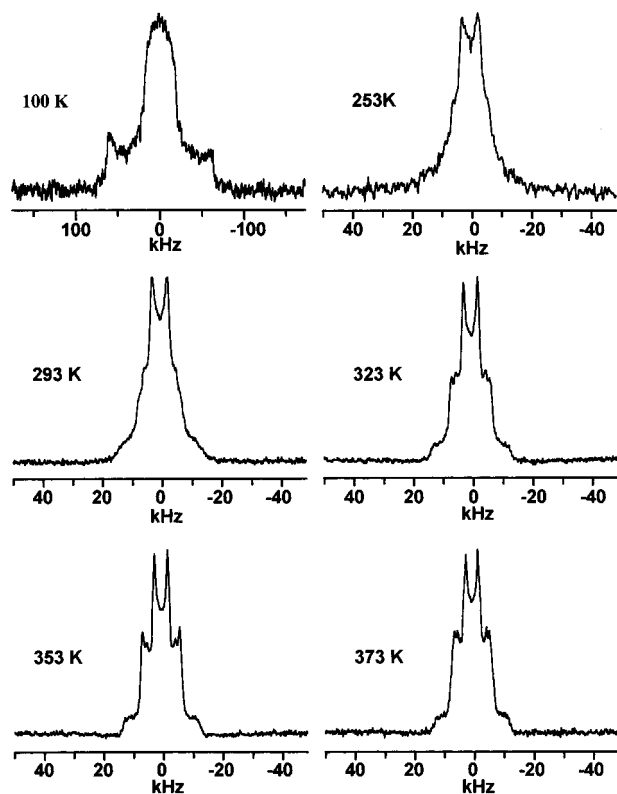


Figure 2. Variation with temperature of the ^2H NMR spectrum of *n*-octane- d_{18} adsorbed on H-ZSM-5 for a loading of 1.8 molecules per unit cell before 1 h of heating at 373 K.

a time τ_1 until it is trapped again in a new equilibrium position (in our case $\tau_0 \gg \tau_1$). Two parameters can be characterized in this model: the mean residence time on a given site τ_0 and the mean jump length.

When the line shape deviates significantly from a Lorentzian profile, an analysis of the QENS spectra in terms of one-dimensional diffusion can be performed.⁷ Such would be the case in ZSM-5 if the molecules move preferably along one channel system.

Results

Analysis of the ^2H NMR Line Shape for *n*-Octane- d_{18} at Loading of 1.8 Molecules per Unit Cell. Figure 2 shows the variation with temperature of the ^2H NMR spectrum of *n*-octane- d_{18} adsorbed in zeolite H-ZSM-5 for a loading of 1.8 molecules per unit cell. The line shape at 100 K is inherent for "rigid" molecules. The CD_3 groups exhibit strongly reduced quadrupole splittings, whereas the methylene groups appear to be immobile. For $T \geq 253$ K, the observed ^2H NMR spectrum represents a superposition of two line shapes. The observed quadrupole splittings of approximately 5 and 14 kHz are close to $1/27$ and $1/9$ of the quadrupole splitting of $3/4Q_0 = 127$ kHz for deuterons of CD_2 groups of *n*-octane- d_{18} at 100 K. Such variations of the observed quadrupole splitting involving factors of 3 for CD_2 deuterons are in agreement with a model where the internal motions of *n*-octane molecules inside the zeolite channels are considered as effective rotations of methylene groups about two adjacent C-C bonds (Figure 1C). In this case, a reduction factor of $1/9$ for the quadrupole splitting is expected (eq 2). In any model of internal rotations (three site jumps or free diffusion) for an *n*-octane molecule, the rotation of terminal methyl deuterons about the 3-fold C- CD_3 axis provides an additional degree of freedom, leading to an additional reduction factor of

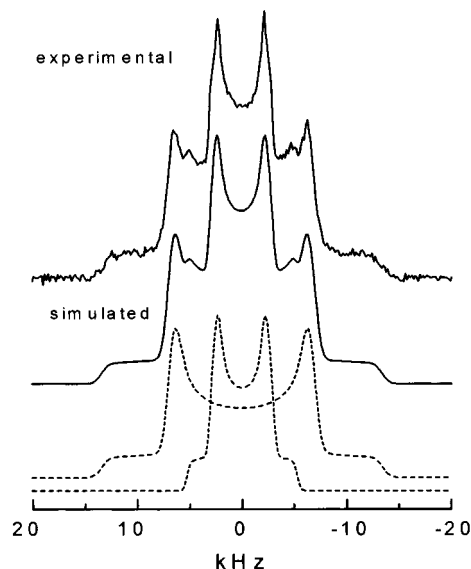


Figure 3. Deconvolution and best fit ($C_Q = 7.05$ kHz, $\eta \approx 0.14$ for CD_3 - groups, and $C_Q = 17.95$ kHz, $\eta \approx 0$ for CD_2 - groups) for the experimental ^2H NMR spectrum at 353 K of *n*-octane- d_{18} adsorbed on H-ZSM-5, before 1 h of heating at 373 K.

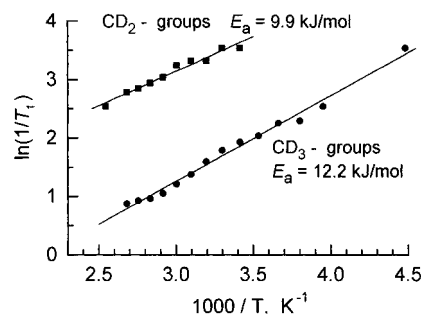


Figure 4. ^2H NMR spin-lattice relaxation data for CD_2 - and CD_3 - groups for *n*-octane- d_{18} adsorbed on H-ZSM-5 at a loading of 1.8 molecules per unit cell.

$1/3$ and to a total factor of about $1/27$. This implies that the motion of the adsorbed *n*-octane molecule, observed by ^2H NMR, displays fast rotations of methylene and methyl groups around two and three C-C bonds, respectively.

A computer deconvolution and parameter fitting of the total spectrum at 373 K is presented in Figure 3. This procedure gives $Q_3 = 7.05$ kHz, $\eta \approx 0.14$ for CD_3 - groups and $Q_2 = 17.95$ kHz, $\eta \approx 0$ for CD_2 - groups. A nonzero value for the asymmetry parameter of CD_3 deuterons as well as a total reduction factor for CD_3 - groups equal to $1/24$ ($1/24 \approx Q_3/Q_0 = 7.05/169.5$) instead of $1/27$ evidence that the real motion of *n*-octane molecules confined in the zeolite framework should be definitely more complex than a suggested set of independent internal rotations. Note that the quadrupole splitting of 5 kHz observed for the methyl deuterons indicates that there is no isotropic reorientation for adsorbed *n*-octane molecule within a time less than the reciprocal value of this splitting, i.e., $\tau_C \gg 2 \times 10^{-4}$ s.

Spin-lattice relaxation times T_1 were measured as a function of temperature in the range 253–373 K for deuterons of both CD_2 and CD_3 groups of adsorbed *n*-octane- d_{18} . The variation of the logarithm of $1/T_1$ as a function of reciprocal temperature ($1/T$) is linear through the whole temperature range studied (Figure 4). The slope of $1/T_1$ indicates that we are operating far from the T_1 minimum, and the quadrupole spin-lattice relaxation is defined by the fast internal motions with charac-

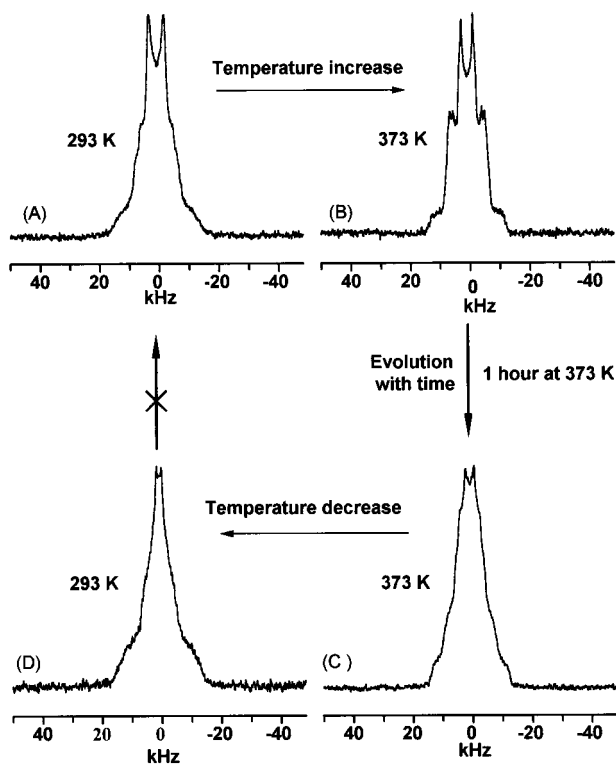


Figure 5. Irreversible change of the ^2H NMR spectrum of n -octane- d_{18} adsorbed on H-ZSM-5 at a loading of 1.8 molecules per unit cell upon 1 h of heating at 373 K.

teristic times τ_C satisfying the condition $\omega_1\tau_C \ll 1$, i.e., $\tau_C \ll 2.6 \times 10^{-9}$ s. At 303 K, the experimental values of the spin-lattice relaxation rates $1/T_1$ for CD_3 - and CD_2 - deuterons are 6.02 and 34.7 s^{-1} . Using eq 6 (with $\eta = 0$ and $Q_0 \approx 170 \text{ kHz}$) as a rough approximation for $1/T_1$ and taking into account that only the rapidly fluctuating component of the quadrupole coupling tensor is responsible for the spin-lattice relaxation, we may estimate that fast internal motions with $\tau_C \geq 1.4 \times 10^{-11}$ s and $\tau_C \geq 8.1 \times 10^{-11}$ s are responsible for the spin-lattice relaxation of CD_3 - and CD_2 - deuterons, respectively. These estimated values of τ_C are in a good agreement with typical values of correlation times for diffusional rotations (jumps) about C-C bonds in hydrocarbons.^{13,41} The activation energies of 12.2 and 9.9 kJ/mol obtained for the methyl and methylene groups are also in keeping with those determined for torsional vibrations in ethane⁴² or predicted for transformations between trans and gauche conformations in other alkanes.⁴³ Note in advance that the local internal motions of CD_n ($n = 2, 3$) groups estimated above $\sim 10^{-11}$ s are much faster than translational jumps between channel sections ($\sim 10^{-9}$ s, vide infra QENS data).

It should be noted that the variation of the NMR spectra is reversible within the temperature range 100–373 K. However, if we keep the zeolite sample with adsorbed n -octane- d_{18} at 353 K or 373 K for a long time (1 h at 373 K or longer at 353 K), then the line shape of the NMR spectrum of n -octane- d_{18} changes. The ^2H NMR line shape for adsorbed n -octane- d_{18} after 1 h of heating at 373 K is depicted in Figure 5C. A further decrease of the temperature leads to a line shape that has nothing in common with the line shape we had at 293 K before increasing the temperature. A subsequent variation of the ^2H NMR spectrum with temperature is shown in Figure 6. The observed NMR line shape is different from the one we had before prolonged heating at 373 K. Changes in the NMR spectrum with temperature are now reversible as shown in

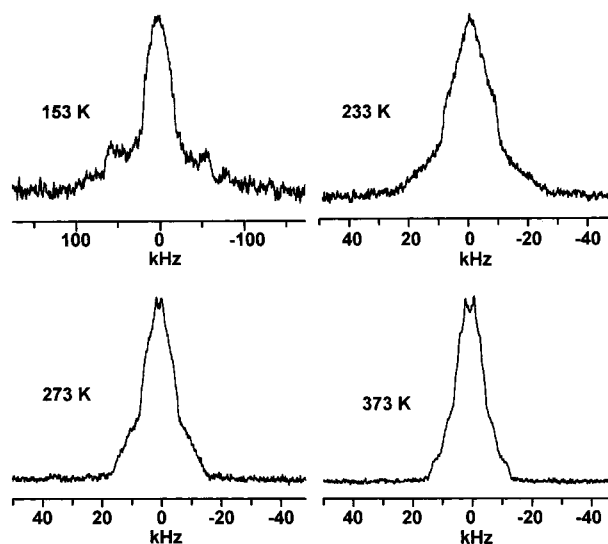


Figure 6. Variation with temperature of the ^2H NMR spectrum for n -octane- d_{18} adsorbed on H-ZSM-5 for a loading of 1.8 molecules per unit cell, after 1 h of heating at 373 K.

Figure 6, but we no longer observe the line shape described above and associated with intramolecular rotations of methyl and methylene groups around two and three C-C axes.

A detailed computer analysis of the final spectrum at 373 K (Figure 5 C) was performed. A straightforward deconvolution of this spectrum is ambiguous. Therefore, to separate reliably the overlapping signals contributing to the spectrum in Figure 5C, we have taken advantage of the difference in spin-lattice relaxation times T_1 for deuterons of CD_3 - and CD_2 - groups of n -octane- d_{18} . By the variation of the time interval t_v between 180° and 90° pulses (sequence *ii*) it was possible to choose the time delay in such a manner that signals either from deuterons of CD_3 - or CD_2 - groups were observed. Figure 7 shows two spectra from CD_3 - or CD_2 - groups separated in inversion-recovery experiments. Simulation of these separate ^2H NMR spectra indicates that each of them is a superposition of two overlapping signals. Therefore, the completely relaxed spectrum in Figure 5C consists of four signals. Using the parameters estimated from the inversion-recovery experiment in Figure 7 as a starting point for the optimization procedure, the values of the quadrupole constants and parameters of anisotropy given in Table 1 were obtained for the overlapping signals. Looking at the data presented in Table 1 one may conclude that there are two different modes of n -octane motion in ZSM-5 at 353–373 K, with a slow (on the ^2H NMR time scale) interchange between them. Upon the basis of the asymmetry parameters presented in Table 1, it is reasonable to assign the line shapes with quadrupole coupling constants $C_Q(\text{CD}_2) = 17.9 \text{ kHz}$ and $C_Q(\text{CD}_3) = 7.0 \text{ kHz}$ to one mode of n -octane motion while those with $C_Q(\text{CD}_2) = 22.1 \text{ kHz}$ and $C_Q(\text{CD}_3) = 6.1 \text{ kHz}$ can be attributed to the second mode.

Thus, after prolonged heating at 373 K, n -octane- d_{18} adsorbed on zeolite ZSM-5 exhibits a motional behavior different from the one observed with ^2H NMR before heating. At least two different modes of molecular motion contributing to the overall ^2H NMR line shape can be distinguished after such heating. It appears that this irreversible transformation of the NMR line shape should be related to the specific system of intersecting straight and zigzag channels of the ZSM-5 zeolite. Therefore we further discuss (*vide infra*, Discussion section) some possible modes of molecular motion inside the channels of the zeolite, which could reasonably satisfy both the observed ^2H NMR

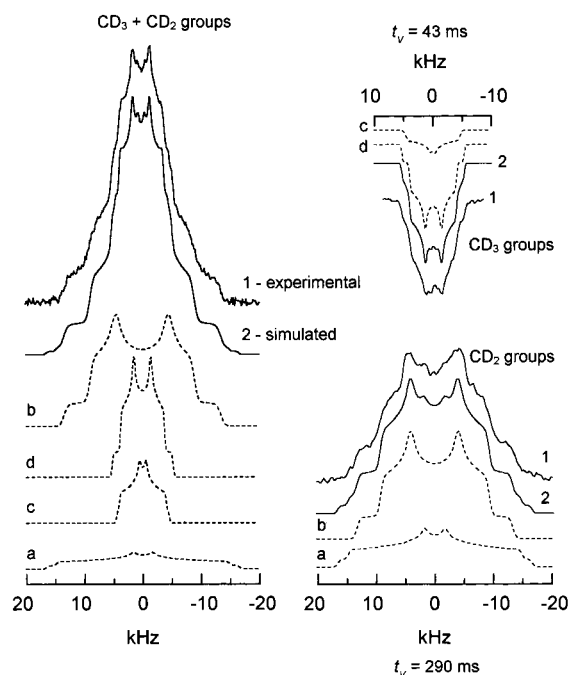


Figure 7. Experimental and simulated ^2H NMR spectra at 373 K from CD_3 - and CD_2 - groups separated in inversion-recovery experiments using different time intervals between 180° and 90° pulses in the pulse sequence ii. The time delays of 43 and 290 ms were used to observe either the spectrum from CD_3 - or CD_2 - groups, respectively. The signals a–d correspond to the signals a–d in Table 1.

TABLE 1. Quadrupole Coupling Constants and Asymmetry Parameters of Signals from *n*-octane- d_{18} Adsorbed in H-ZSM-5 at 353 K after Preliminary 1 h of Heating the Sample at 373 K (loading: 1.8 molecules per unit cell)^a

	group	$C_Q = e^2qQ/h$, kHz	η	relative intensity
a	CD_2 -	22.1	0.80	0.1
b	CD_2 -	17.9	0.33	0.55
c	CD_3 -	6.1	0.77	0.11
d	CD_3 -	7.0	0.44	0.24

^a The signals a–d correspond to the signals a–d in Figure 7.

spectra at the loading of 1.8 molecule per unit cell and their changes upon heating.

Analysis of the ^2H NMR Line Shapes for *n*-Octane- d_{18} at Loadings of 3.5 and 5.3 Molecules per Unit Cell. After an increase of *n*-octane loading up to 3.5 molecules per unit cell, the solidlike line shape corresponding to the internal rotations of CD_n ($n = 2, 3$) groups around C–C bonds is also observed at 253 and 353 K (Figure 8). However, a narrow liquidlike signal, related to isotropic reorientation of adsorbed *n*-octane with $\tau_C < 2 \times 10^{-4}$ s, appears at 253 K. The relative intensity of this narrow signal increases with temperature, while the intensity of the solidlike signal decreases. The spectrum variation within the temperature range 100–353 K is reversible, which indicates that an equilibrium between *n*-octane molecules reorienting “anisotropically” and “isotropically” exists. A further increase of the *n*-octane loading up to 5.3 molecules per unit cell (Figure 9) results in a further redistribution of the NMR signal intensity between the solid and liquidlike signals in favor of the latter one. At 283 K, about 50% of the total NMR signal intensity belongs to the liquidlike signal. The slope of $1/T_1$ for both CD_2 - and CD_3 - groups (Figure 10) indicates that we are on the *fast* motion side of the T_1 minimum. Moreover, the T_1 values nearly coincide with those for the methyl group in Figure 4. Consequently, we may suppose that the spin–lattice relaxation of the liquidlike signal is induced, as in the previous case,

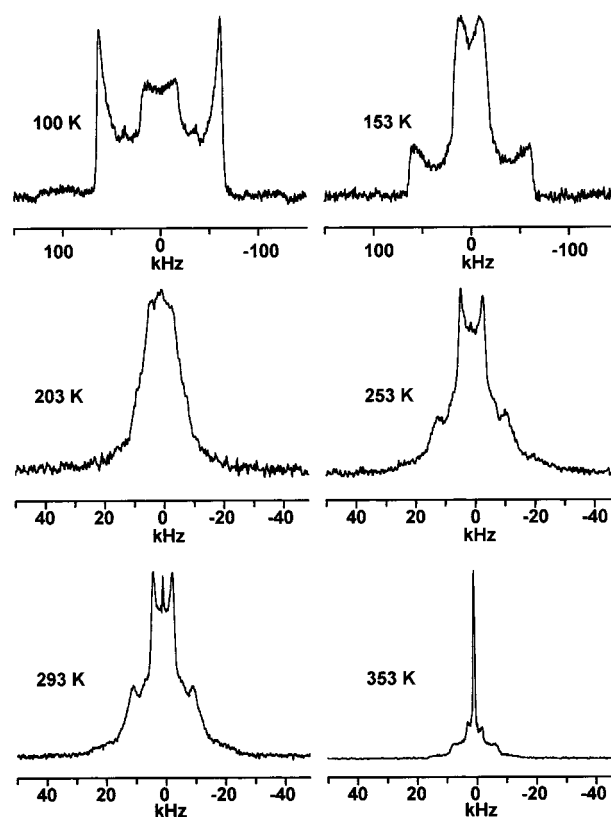


Figure 8. Variation with temperature of the ^2H NMR spectrum of *n*-octane- d_{18} adsorbed on H-ZSM-5 for a loading of 3.5 molecules per unit cell.

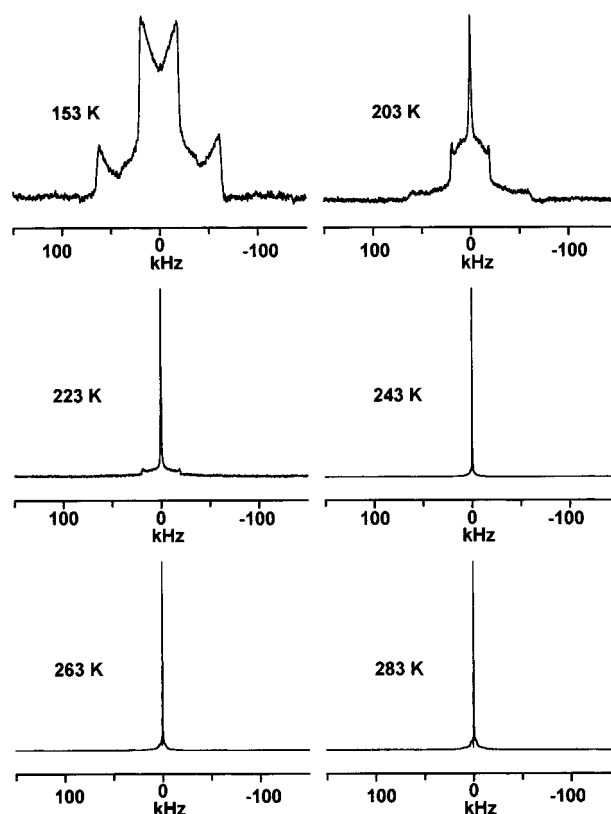


Figure 9. Variation with temperature of the ^2H NMR spectrum of *n*-octane- d_{18} adsorbed on H-ZSM-5 for a loading of 5.3 molecules per unit cell.

by the rapid component of *intramolecular* motion and eq 6 should be applied for an estimation of the correlation time for

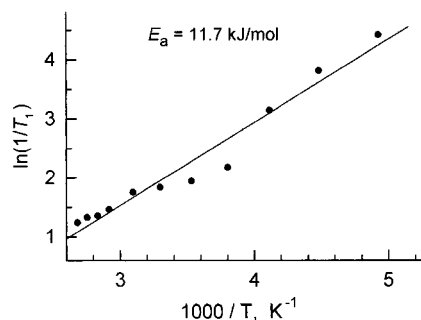


Figure 10. ^2H NMR spin-lattice relaxation data for CD_2 - and CD_3 - groups of n -octane- d_{18} adsorbed on H-ZSM-5 at a loading of 5.3 molecules per unit cell. Both CD_2 - and CD_3 - groups exhibit the same values of T_1 .

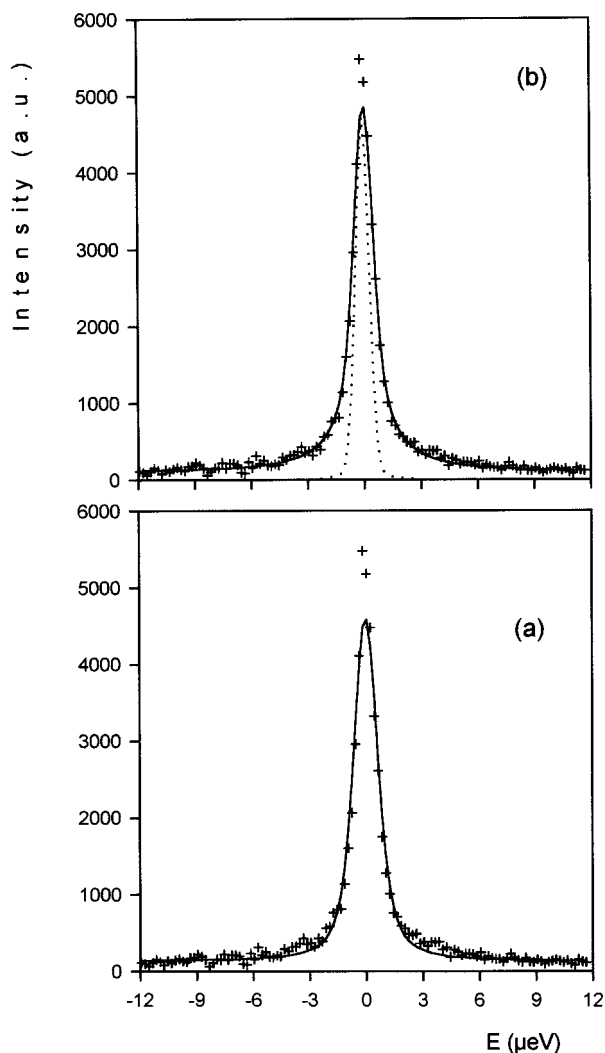


Figure 11. Comparison between experimental (+) and calculated (full line) QENS spectra obtained for n -octane in ZSM-5 at 300 K: (a) fit with an isotropic diffusion, (b) fit with a one-dimensional diffusion. The dotted line represents the resolution function ($Q = 0.87 \text{ \AA}^{-1}$).

isotropic reorientation τ_C . The estimation at 303 K from $1/T_1 = 6.3 \text{ s}^{-1}$ gives a value of $\tau_C = 1.5 \times 10^{-11} \text{ s}$. An apparent activation energy E_a estimated from the temperature dependence of the slope of $1/T_1$ is 11.7 kJ/mol (Figure 10). Both E_a and τ_C are in good agreement with the activation energies found for the *local internal* motions of the methyl and methylene groups at a loading of 1.8 molecules per unit cell.

Analysis of QENS Spectra. On comparing the experimental spectra with the resolution function, e.g. Figure 11, it is clear

that large broadenings are measured, which means that the molecules move on a time scale of $\sim 1 \text{ ns}$. These broadenings correspond to the long-range translational motion since the rotational or local motions involve much larger energy transfers.⁴⁰ The QENS spectra were fitted with two models: (i) an isotropic diffusion and (ii) a one-dimensional (1D) diffusion. The 1D model gave the best fits to the data, this is illustrated in Figure 11. For a momentum transfer of 0.87 \AA^{-1} , the 1D diffusion model yielded a weighted profile R factor, R_{wp} , of 14.4%, while the 3D model gave $R_{wp} = 19.7\%$.

All the experimental spectra obtained at different Q values could be fitted simultaneously with a 1D jump diffusion model, convoluted with the instrumental resolution. Values of 8.5 \AA and $3.0 \times 10^{-9} \text{ s}$ were derived for the mean jump length and mean residence time, respectively. This corresponds to a value of $12.0 \times 10^{-11} \text{ m}^2/\text{s}$ for the 1D diffusion coefficient at 300 K (the mean diffusivity is of $4.0 \times 10^{-11} \text{ m}^2/\text{s}$). At small Q values, a mean diffusivity could also be obtained by fitting the isotropic Fick's law to the data. This model is valid in this Q range because the diffusion occurs after a large number of jumps and because the broadenings are small compared with the instrumental resolution.⁴⁴ Comparable values of the mean diffusivities were obtained, within experimental error. In this study, the error on the diffusion coefficient is estimated to be of a factor of 2.

Discussion

The Motion of Adsorbed n -Octane before Prolonged Zeolite Heating at 373 K. It follows from the obtained results that the ^2H NMR and QENS techniques allow us to get a deep insight into the real dynamics of n -octane inside a constrained area of the channel system of ZSM-5 zeolite. The peculiarity of the observed ^2H NMR line shape for adsorbed n -octane- d_{18} and its evolution upon keeping the zeolite sample at 373 K allows us to discriminate between the localization and dynamics of n -octane molecules inside the zeolite channel system just after adsorption and after subsequent heating. It results from the NMR line shape analysis that the molecular motion of adsorbed n -octane, responsible for the spin-lattice relaxation, is fast ($\tau_C \approx 10^{-11} \text{ s}$) and manifests itself in the ^2H NMR spectrum as rotations of methyl and methylene groups simultaneously about three and two C-C bonds, without isotropic reorientation of the molecule with a characteristic time faster than $\sim 10^{-4} \text{ s}$. The same order of magnitude for the correlation time, $\sim 10^{-11} \text{ s}$, has been found by QENS for n -hexane in ZSM-5.⁴⁰ It is known from molecular simulation work on hydrocarbons in silicalite that the channel intersections are high-energy barriers for adsorbed alkanes, because in the channel intersections the hydrocarbon chain loses its energetically favorable contacts with the framework oxygen atoms.^{20,22} Therefore, the segments of either zigzag or straight channels are more preferable than the channel intersections for the localization of n -octane. Nevertheless, it is evident that neither the channels with a diameter of ca. 5.5 \AA nor the intersection region with a dimension of ca. 8 \AA possess sufficient space for *independent* (as compared with the isolated molecule) rotations of the methylene or methyl groups simultaneously around two or three axes. Certainly, the mechanism adequate to describe the observed motion of CD_2 - and CD_3 - groups should include some *coupled* motion (rotational and librational) of all CD_n - ($n = 2, 3$) groups of the hydrocarbon skeleton of the n -octane- d_{18} molecule. One cannot exclude that the 8 \AA channel intersection plays some role in providing the space for the observed CD_n - groups rotational motion. Indeed, the rotation

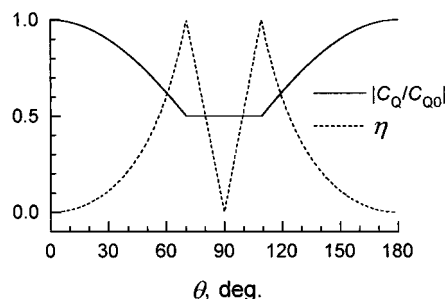


Figure 12. Predicted dependence of effective values for η and C_Q vs θ angle between directions of axial axis of quadrupole tensor ($\eta = 0$) in the case of rapid exchange between two equally populated sites.

of the methyl groups simultaneously around two axes is quite possible in the channel intersection, e.g., for adsorbed *tert*-butyl alcohol.¹⁶

From the QENS measurements carried out at 300 K, an average diffusion coefficient of $4.0 \times 10^{-11} \text{ m}^2/\text{s}$ is obtained. In accordance with the NMR data, this means that in the course of translational diffusion, the *n*-octane molecule also exhibits multiple combined rotations of CH_n ($n = 2, 3$) groups, which are reflected in the NMR spectrum (Figure 2, $T = 253\text{--}373 \text{ K}$) and may be indeed related with fast interconversions between *trans* and *gauche* conformations in the adsorbed alkane molecule. The mean residence time τ_C of the *n*-octane molecule inside a channel, as found by QENS, is $\tau_C = 3 \times 10^{-9} \text{ s} \ll \tau_{\text{NMR}}$. As follows from the ^2H NMR analysis of *n*-octane- d_{18} motion for a loading of 1.8 molecules per unit cell, there may be an isotropic averaging of the NMR line shape only on the time scale of $2 \times 10^{-4} \text{ s}$. During this time interval, an *n*-octane molecule experiences a few thousand hops but still keeping the memory along the channel direction. This implies that *n*-octane reorients rapidly inside the zeolite framework on the ^2H NMR time scale ($\tau_{\text{NMR}} \approx 5 \times 10^{-6} \text{ s}$), but this motion is *significantly anisotropic*.

One can envisage at least three types of motion for *n*-octane captured by the ZSM-5 pore system, namely, along the straight channels, along the tortuous zigzag channels, and along a tortuous path between the straight and zigzag channels via the intersection region. If we assume that *n*-octane moves rapidly either exclusively along the zigzag channels or along a tortuous path between the straight and zigzag channels, then either of these modes should *change the direction of its translational motion* in the channel intersections. In this case, the observed ^2H quadrupole coupling tensor should be averaged by the hops of the *n*-octane molecule between two sites either with an angle close to the zigzag channels angle ($\theta \approx 112.6^\circ$) or with an angle ($\theta \approx 90^\circ$) between the straight and zigzag channels. The theoretical dependence of the effective anisotropy parameter η and of the effective quadrupole constant C_Q on the angle θ is shown in Figure 12 in the case of exchange between two equally populated sites and an initially axial quadrupole tensor. On the basis of this plot, we note that a significant anisotropy $\eta \approx 0.86$ is expected for jumps between segments of the zigzag channels. This is in contrast with the experimental results, and we should exclude this type of motion for adsorbed *n*-octane before prolonged zeolite sample heating at 373 K. Despite the fact that for $\theta = 90^\circ$ the predicted value of η is zero, the motion of the alkane between straight and zigzag channels is unlikely for some reasons. First, the conclusion on zero η value for $\theta = 90^\circ$ is valid only for hops between *equally* populated sites, and second, this motion is inconsistent with the redistribution of *n*-octane in the zeolite channel system after heating at 373 K (*vide infra*). Therefore, the translational motion of *n*-octane

along the straight channels (most likely in the form of jumps between neighboring channel segments) is best suited for the description of ^2H NMR experimental data for *n*-octane at a loading of 1.8 molecules per unit cell before prolonged heating.

Note that the diffusion at any rate along the *straight* ideal cylindrical channel includes averaging of the quadrupole tensor only by the rotation about the channel direction. This results in $\eta = 0$ and a nonzero value of the effective quadrupole constant C_Q . For the real straight channel of the ZSM-5 zeolite, deviations from the axiality induced, e.g., by the intersections with the zigzag channels, may be the reason why a small nonzero asymmetry parameter $\eta \approx 0.14$ is observed.

Finally, we conclude that the ^2H NMR spectra in Figure 2 in the temperature range 253–373 K correspond to *n*-octane located in the straight channels of the zeolite and diffusing along their direction with a diffusion coefficient $D = 12.0 \times 10^{-11} \text{ m}^2/\text{s}$ at 300 K. The mean diffusivity of *n*-octane in ZSM-5 ($4.0 \times 10^{-11} \text{ m}^2/\text{s}$) is 1 order of magnitude lower than the one derived for *n*-hexane in the same zeolite ($4.5 \times 10^{-10} \text{ m}^2/\text{s}$).⁴⁰ This is in contrast with recent simulations which predict a small decrease²¹ or an increase²² of the mean diffusivity of *n*-octane in silicalite, relative to *n*-hexane. It appears that these simulations, performed with a fixed framework and the united atoms model, are able to correctly reproduce the dynamics of short alkanes, but they are less precise for long alkanes. In the course of translational motion, some coupled “rotational” motions of all CH_n ($n = 2, 3$) groups of the hydrocarbon skeleton in the molecule take place, which may correspond to fast interconversions between different conformations of the *n*-octane molecule and which are reflected in the ^2H NMR spectra as fast rotations of the separate CD_2 - and CD_3 - groups simultaneously around two and three C–C bonds in the molecule.

The Motion of Adsorbed *n*-Octane after Heating at 373 K. It is well-known that the lattice of ZSM-5 exhibits a phase transition either at elevated temperature or upon loading of some adsorbates. Therefore, one could attribute the observed change of the dynamic behavior of *n*-octane at 373 K to a possible phase transition in the lattice of the zeolite. The changes between monoclinic and orthorhombic forms occur at ca. 356 K for silicalite⁴⁵ but at lower temperatures for ZSM-5. It was also shown in ref 45 that in the case of loading of some adsorbates, e.g., *p*-xylene in the amount of 2 molecules/unit cell, the monoclinic form transforms into the orthorhombic form at 295 K. This implies that in our experiments at temperatures higher than room temperature the zeolite lattice already exists in the orthorhombic form and the transformation of the NMR line shape at 373 K cannot be related to the possible phase transition. If, nevertheless, the phase transition occurs, it results only in slight changes in the shape of the zeolite channel,⁴⁶ and therefore, the phase transition could only slightly influence the molecular motion of adsorbed molecules. The changes cannot be related either to the possible isomerization of linear *n*-octane or to the formation of branched alkanes, which could exhibit molecular motions different from those of *n*-octane. Indeed, our ^{13}C MAS NMR experiment has indicated that there is no isomerization of *n*-octane upon heating at 373 K for 1 h. Therefore, we believe that the appearance of two types of molecular motion for adsorbed *n*-octane after heating at 373 K, which are essentially different from the single type of motion observed before heating, should be related to the activated penetration of sorbate molecules from the straight to the zigzag channels, where *n*-octane localization may then become thermodynamically preferable. The phenomenon of irreversible redistribution of *n*-octane molecules, formerly located in the

straight channels, over the whole channel system of the zeolite does not seem to be unusual,^{47,48} except that we are able to follow it on the *molecular* level by monitoring the transformation of the ²H NMR spectrum at 373 K.

In accordance with theoretical predictions,^{21,22} *n*-octane redistributed inside the zeolite channel system and located in both straight and zigzag channels may further exhibit three modes of translational motion: movements along the straight, movements along the zigzag channels, as well as movements from the straight to the zigzag channels or vice versa. We try to interpret below the observed ²H NMR line shapes in relation to these three possible modes of *n*-octane translational motion.

Theoretical results predict very fast (hundreds of picoseconds²²) exchange for an *n*-octane molecule between its location in straight and zigzag channels in the process of translational motion. QENS measurements indicate that the residence time of the molecule in a channel is 3.0×10^{-9} s, provided that the diffusion of the molecule is of a similar rate as it was before heating at 373 K, when the molecules were located only in the straight channels. Therefore, one can assume that the observed line shapes should reflect an averaging of the ²H quadrupole tensor due to jumps between the straight and zigzag channels or exclusively between zigzag channels. It is reasonable to assume that notable values of asymmetry parameters obtained after heating at 373 K originate from an uniaxial averaging of the quadrupole tensor in the process of jumps between two energetically equivalent adsorption sites. One may assume that local averaging (internal rotations of CD_{*n*}- groups and other motions which have been observed before heating and which take place during the time interval between jumps) at each of the adsorption sites inside the channels leads to a quadrupole tensor close to axial. Then, it is possible to estimate from the experimental values of η and C_Q both the angle θ (θ is the angle between end-to-end vector of the molecule before and after the jump) and the value of the quadrupole coupling constant C_Q^0 averaged only by local movements at a given adsorption site, i.e., without averaging by jumps between adjacent adsorption sites. The predicted dependence of the η and C_Q effective values vs θ angle for initially axial quadrupole tensor is shown in Figure 12. On the basis of this plot and on the value $\eta(\text{CD}_2) = 0.80$, we find $\theta(\text{CD}_2) = 66^\circ$ and $\theta(\text{CD}_3) = 65.2^\circ$ from $\eta(\text{CD}_3) = 0.77$. It is interesting to notice that the value of $180^\circ - \theta \approx 114\text{--}115^\circ$ is close to the angle computed from the experimental ZSM-5 structure⁴⁹ between neighboring segments of zigzag channels (112.6°). Finally, using the θ angles and the experimental values of $C_Q(\text{CD}_2) = 22.1$ kHz and $C_Q(\text{CD}_3) = 6.1$ kHz (Table 1), it is possible to estimate that $C_Q^0(\text{CD}_2) = 39.8$ kHz and $C_Q^0(\text{CD}_3) = 10.8$ kHz. Thus, we conclude that the observed line shape with $\eta(\text{CD}_2) = 0.80$ and $\eta(\text{CD}_3) = 0.77$ corresponds to the tortuous movement of the *n*-octane molecule along the zigzag channels. Note that there is also an alternative formal set of parameters giving the same values of the quadrupole tensor asymmetry $\eta(\text{CD}_2) = 0.80$ and $\eta(\text{CD}_3) = 0.77$. For this set, $\theta(\text{CD}_2) = 74.5^\circ$, $C_Q^0(\text{CD}_2) = 44.2$ kHz, $\theta(\text{CD}_3) = 75.1^\circ$, $C_Q^0(\text{CD}_3) = 12.2$ kHz. However, it is difficult to assign these values to any of the possible modes of motion into the zeolite framework.

The estimates of C_Q^0 and θ for the other signals with a smaller anisotropy $\eta(\text{CD}_2) = 0.33$ and $\eta(\text{CD}_3) = 0.44$ give us also two possible sets of parameters: $\theta(\text{CD}_2) = 48^\circ$, $C_Q^0(\text{CD}_2) = 23.8$ kHz, $\theta(\text{CD}_3) = 53.7^\circ$, $C_Q^0(\text{CD}_3) = 10.1$ kHz for the former set and $\theta(\text{CD}_2) = 83.7^\circ$, $C_Q^0(\text{CD}_2) = 35.8$ kHz, $\theta(\text{CD}_3) = 81.6^\circ$, $C_Q^0(\text{CD}_3) = 14.0$ kHz for the latter set. The values of θ in the latter set are close to the angle 90° between the

directions of the straight and zigzag channels, which means that, in principle, two other line shapes with smaller values of η contributing to the total signal in Figure 7 may reflect an interchange between the straight and zigzag channels. It should be noted that the calculated values of $C_Q^0(\text{CD}_2)$ and $C_Q^0(\text{CD}_3)$ do not correspond to the effective internal rotations around C–C axes we had for adsorbed *n*-octane before heating. To accept this model one should assume that after the molecule redistribution inside the zeolite framework and the beginning of the molecule interchange between the straight and zigzag channels, the intramolecular modes (there are many internal rotational degrees of freedom) of the molecule at an adsorption site inside the channels are different from those observed for the molecules located exclusively in the straight channels before prolonged heating at 373 K. Indeed, as can be seen from the comparison of Figures 3 and 7, there is no line shape in Figure 7 which could be attributed to the movement of *n*-octane along the straight channels with simultaneous fast *coupled* rotations of CH_{*n*} groups after molecule redistribution at 373 K.

From a qualitative point of view, the movement of *n*-octane from the straight to the zigzag channels should be less favorable than the motion along the straight channels only, because the former implies an additional entropy and energetic restrictions connected with the necessity for the moving molecule to conform the contour of the channels and to significantly change its conformation during the interchannel movement. Therefore, we believe that the data with the smaller values of the asymmetry parameter may be alternatively interpreted. Attention should be paid to the fact that for the motion with the smaller asymmetry parameters, the quadrupole coupling constants are close to the values $C_Q(\text{CD}_2) = 17.95$ kHz and $C_Q(\text{CD}_3) = 7.05$ kHz, which were observed for *n*-octane molecules located in the straight channels before heating at 373 K. Only the asymmetry parameters are increased from 0 and 0.14 up to 0.33 and 0.44 after heating, respectively. Therefore, it is possible to consider this type of motion as the motion along the straight channel that we had before heating at 373 K but disturbed by collisions with the other *n*-octane molecules diffusing along the zigzag channels. Indeed, before heating, the movement along the straight channels presumably occurs without collisions with the molecules located in the zigzag channels. After heating, some part of the *n*-octane molecules penetrate into the zigzag channels and the possibility of molecular collisions appears. van der Waals forces acting during collisions are definitely uniaxial; they disturb close to axial (before zeolite heating) averaging of the quadrupole tensor about the straight channel axis, leading to the appearance of a non-zero asymmetry parameter.

The following additional arguments also exist against the model of 90° jumps from straight to zigzag channels. The relative intensities in Table 1 indicate that about 20% of the molecules translate along the zigzag channels while 80% make the supposed 90° bends. This would imply that a molecule residing in the zigzag channel prefers to make the difficult transition to the straight channel over making the much easier translational motion along the zigzag channel. Likewise, the supposed model implies that every molecule in the straight channel prefers to round the corners over moving along the straight channel. Moreover, as follows from the theoretical dependence of η (Figure 12), a model of 90° jumps with η close to zero may be valid only for flips between two equally populated sites. Since there is no symmetry between the zigzag and the straight channel, it is unlikely that the populations are equal in this case. Hence, small values of η may not be a strong argument for the 90° jump model.

Thus, we finally conclude that upon heating at 373 K, the molecules formerly located in the straight channels become redistributed over the straight and zigzag channels. After redistribution, the translational motion of *n*-octane consists of two independent motions. One of them represents the movement along the tortuous zigzag channel. The other one represents most probably the movement along the straight channels disturbed by collisions with other *n*-octane molecules located in the zigzag channels.

The Motion of Adsorbed *n*-Octane at Higher Loadings.

The transformation from well-structured NMR spectra at low loadings to the motional averaged singlet line at higher loadings can be described in terms of decorrelation of molecular orientation caused by an increasing rate of sorbate–sorbate collisions with increasing loading. It is obvious that sorbate–sorbate collisions should result in the averaged singlet in the NMR spectrum, irrespective of specific features of internal motions in the molecule. The phenomenon of orientational decorrelation induced by collisions, e.g., for methane in silicalite, was studied experimentally by QENS³⁸ and theoretically using MD simulations (see review⁴³ and references therein). As for long-chain *n*-alkanes, only a few theoretical and experimental investigations of their mobility and loading dependence either in ZSM-5 or in silicalite exist. Theoretical estimations of diffusion coefficients and end-to-end vector self-correlation decay were performed for *n*-hexane in silicalite for loadings up to four molecules per unit cell.^{20,50} The only known theoretical estimates of time constants for molecular rearrangement of *n*-octane in silicate were performed for a loading of a few molecules.²² Unfortunately, the study of normalized end-to-end vector decorrelation rates does not give us valuable information on the C–D bond direction decorrelation (more exactly, on the ²H quadrupole coupling tensor components). Special, more complete MD simulations without the united atoms potential model approximation used in ref 22 are necessary. Characteristic times of different component end-to-end vector decorrelation reported for *n*-octane²² are less than 10^{−9} s for all temperatures and all loadings. This corresponds to a fast, on the ²H NMR time scale, interchange rate between the zigzag and straight channels of *silicalite* and is incompatible with our experimental results at low *n*-octane loading (1.8 molecules per unit cell) in ZSM-5 before heating at 373 K. *Silicalite*⁵¹ and ZSM-5²⁴ channel systems are similar, and in the case of fast exchange between all accessible positions in the zeolite lattice, we should observe only one mode of *n*-octane motion, which is in contrast with the observation of two modes after heating at 373 K (for 1.8 molecules per unit cell). Thus, we conclude that upon increasing the loading from 1.8 to 5.3 molecules per unit cell, the decorrelation time for C–D bond direction for the liquidlike component of the spectrum decreases from the value $\tau_C \gg 2 \times 10^{-4}$ s to $\tau_C \leq 10^{-4}$ s (vide supra, Results section). In addition, it is possible to estimate a low limit for τ_C from the experimental line width and the spin–lattice relaxation rate, deliberately neglecting the contributions from *internal* motions and all other contributions to these values, using eqs 4 and 5, which are valid only for isotropic reorientation. It follows from the experimental value $\Delta\nu_{1/2} = 330$ Hz at 303 K and eq 4 that the orientational decorrelation time is $\tau_{Cmin} \approx 6 \times 10^{-9}$ s. Similarly, from the experimental value of $T_1 = 159$ ms at 303 K and eq 5, we have $\tau_{Cmin} \approx 1.8 \times 10^{-7}$ s. Certainly, this is only a crude estimate of the low limit of orientational decorrelation time. Nevertheless, it is remarkable that these values are in agreement with the suggestion that orientational decorrelation, leading to the observed singlet line in ²H NMR, is caused by sorbate–sorbate

collisions. Remember that the mean residence time of the *n*-octane molecule inside the channel segment, derived from the QENS data, is 3.0×10^{-9} s at 300 K, i.e., smaller or of the same order of magnitude as τ_{Cmin} . It should be emphasized here that the orientational decorrelation time τ_{Cmin} just estimated represents τ_C for an isotropic reorientation of the alkane molecule *as a whole*, it differs from τ_C for *local internal* motions of the CD_{*n*}, which was estimated earlier to be $\sim 10^{-11}$ s for both low and high loadings (vide supra) and which in fact corresponded to the rotational correlation time τ_R .

Conclusion

The following conclusions can be drawn from the ²H NMR and QENS studies about the adsorption and dynamics of *n*-octane inside the channel system of zeolite ZSM-5. The peculiarity of the dynamic behavior of *n*-octane adsorbed in ZSM-5 depends on the loading. Upon exposure under vacuum of the ZSM-5 sample at room temperature to the vapor of *n*-octane, corresponding to a loading of 1.8 molecules per unit cell, the adsorption of this linear alkane occurs exclusively inside the straight channels of the zeolite lattice. *n*-Octane molecules located in the straight channels of the zeolite diffuse essentially along the direction of the straight channels with a diffusion coefficient $D = 12.0 \times 10^{-11}$ m²/s at 300 K. In the course of translational motion along the straight channels, some coupled rotational or librational motions of all CH_{*n*}– (*n* = 2, 3) groups of the hydrocarbon skeleton in the molecule take place, which may correspond to the fast interconversions between *trans* and *gauche* conformations in the adsorbed alkane molecule. This “rotational” motion is *reflected* in the ²H NMR spectra as fast rotations of the separate methylene and methyl groups simultaneously around two and three C–C bonds. Upon heating at 373 K for 1 h, *n*-octane molecules formerly located in the straight channels become redistributed over the straight and zigzag channels. Subsequent translational motion of *n*-octane consists of two independent modes of motion. One of them represents the movement along the tortuous zigzag channel. Another mode of translational motion represents the movement along the straight channels. This movement of the molecule is disturbed by collisions with the other molecules located mainly in the zigzag channels and in part at the channel intersections. For loadings equal to or higher than 3.5 molecules per unit cell, the molecules show isotropic reorientation inside the zeolite channel system, which may arise from collisions of the molecules at the channel intersections, thereby changing the direction of its translational movement.

Acknowledgment. The authors express their gratitude to Prof. V. N. Parmon for valuable comments and interest to the work and Dr. V. N. Romannikov for chemical and XPD analyses on the H-ZSM-5 sample. The neutron experiments were performed at the Institut Laue-Langevin, Grenoble, France. We thank one of the referees for valuable comments. This research was made possible with financial support from INTAS (Grant No. 96-1177).

References and Notes

- (1) Satterfield, C. N. *Heterogeneous Catalysis in Practice*; McGraw-Hill: New York, 1980.
- (2) Yang, R. T. *Gas Separation in Adsorption Processes*; Butterworth Publishers: Stoneham, MA, 1987.
- (3) Karger, J.; Ruthven, D. M. *Diffusion in Zeolites and Other Microporous Solids*; Wiley-Interscience: New York, 1992.
- (4) Chen, N. Y.; Degnan, T. F., Jr.; Smith, C. M. *Molecular Transport and Reactions in Zeolites. Design and Application of Shape Selective Catalysts*; VCH Publishers: Weinheim, 1994.

- (5) Dwyer, J. *Nature (London)* **1989**, 339, 174.
- (6) Heink, W.; Karger, J.; Pfeifer, H.; Stallmach, F. *J. Am. Chem. Soc.* **1990**, 112, 2175.
- (7) Jobic, H.; Hahn, K.; Kärger, J.; Bée, M.; Tuel, A.; Noack, M.; Girnus, I.; Kearley, G. J. *J. Phys. Chem.* **1997**, 101, 5834.
- (8) Jobic, H.; Renouprez, A.; Bée, M.; Poinssignon, C. *J. Phys. Chem.* **1986**, 90, 1059.
- (9) Czjzek, M.; Jobic, H.; Bée, M. *J. Chem. Soc., Faraday Trans.* **1991**, 87, 3455.
- (10) Hasha, D. L.; Miner, V. W.; Garces, J. M.; Rocke, S. C. In *Catalysts Characterization Science*; Deviney, M. L., Gland, J. L., Eds.; ACS Symposium Series 288; American Chemical Society: Washington, DC, 1985; pp 485.
- (11) Eckman, R. R.; Vega, A. J. *J. Phys. Chem.* **1986**, 90, 4679.
- (12) Newsam, J. M.; Silbernagel, B. G.; Garcia, A. R.; Hulme, R. J. *Chem. Soc., Chem. Commun.* **1987**, 664.
- (13) Silbernagel, B. G.; Garcia, A. R.; Newsam, J. M.; Hulme, R. J. *J. Phys. Chem.* **1989**, 93, 6506.
- (14) Vega, A. J.; Luz, Z. *J. Phys. Chem.* **1987**, 91, 365. Vega, A. J.; Luz, Z.; *J. Phys. Chem.* **1987**, 91, 374.
- (15) Kustanovich, I.; Fraenkel, D.; Luz, Z.; Vega, S.; Zimmermann, H. *J. Phys. Chem.* **1988**, 92, 4134.
- (16) Stepanov, A. G.; Maryasov, A. G.; Romannikov, V. N.; Zamaraev, K. I. *Magn. Reson. Chem.* **1994**, 32, 16.
- (17) Abragam, A. *The Principles of Nuclear Magnetism*; Oxford University Press: Oxford, 1961.
- (18) Speiss, H. W. Rotation of Molecules and Nuclear Spin Relaxation. In *NMR Basic Principles and Progress*; Diehl, P., Fluck, E., Kosfeld, R., Eds.; Springer-Verlag: New York, 1978; Vol. 15, p 55.
- (19) Mehring, M. Principles of High-Resolution NMR in Solids. In *NMR Basic Principles and Progress*; Diehl, P., Fluck, E., Kosfeld, R., Eds.; Springer-Verlag: New York, 1976; Vol. 11.
- (20) June, R. L.; Bell, A. T.; Theodorou, D. N. *J. Phys. Chem.* **1992**, 96, 1051.
- (21) Maginn, E. J.; Bell, A. T.; Theodorou, D. N. *J. Phys. Chem.* **1996**, 100, 7155.
- (22) Runnebaum, R. C.; Maginn, E. J. *J. Phys. Chem. B* **1997**, 101, 6394.
- (23) Chang, C. D. *Catal. Rev. Sci. Eng.* **1983**, 25, 1.
- (24) Kokotailo, G. T.; Lawton, S. L.; Olson, D. H.; Meier, W. M. *Nature (London)* **1978**, 272, 437. Olson, D. H.; Kokotailo, G. T.; Lawton, S. L.; Meier, W. M. *J. Phys. Chem.* **1981**, 85, 2238.
- (25) Romannikov, V. N.; Mastikhin, V. M.; Hocevar, S.; Drzaj, B. *Zeolites* **1983**, 3, 313.
- (26) Powles, J. G.; Strange, J. H. *Proc. Phys. Soc.* **1963**, 82, 6. Davis, J. H.; Jeffery, K. R.; Bloom, M.; Valic, M. I.; Higgs, T. P. *Chem. Phys. Lett.* **1976**, 42, 390.
- (27) Farrar, T. C.; Becker, E. D. *Pulse and Fourier Transform NMR. Introduction to Theory and Methods*; Academic Press: New York and London, 1971.
- (28) Smith, I. C. P. Deuterium NMR. In *NMR of Newly Accessible Nuclei*; Laszlo, P., Ed.; Academic Press: London, 1983; Vol. 2, p 1.
- (29) Jelinski, L. W. Deuterium NMR of Solid Polymers. In *High-Resolution NMR Spectroscopy of Synthetic Polymers in Bulk (Methods and Stereochemical Analysis)*; Komoroski, R. A., Ed.; VCH Publishers: New York, 1986; Vol. 7, p 335.
- (30) Barnes, R. G. *Adv. Nucl. Quadrupole Reson.* **1974**, 1, 335.
- (31) Stockton, G. W.; Polnaszek, C. F.; Tulloch, A. P.; Hasan, F.; Smith, I. C. P.; *Biochemistry* **1976**, 15, 954.
- (32) Boddenberg, B.; Grosse, R. Z. *Naturforsch., Teil A* **1986**, 41, 1361.
- (33) Rinne, M.; Depireux, J. *Adv. Nucl. Quadrupole Reson.* **1974**, 1, 357.
- (34) Mantsch, H. H.; Saito, H.; Smith, I. C. P. *Prog. Nucl. Magn. Reson. Spectrosc.* **1977**, 11, 211.
- (35) Schwartz, L. J.; Meirovitch, E.; Ripmeester, J. A.; Freed, J. H. *J. Phys. Chem.* **1983**, 87, 4453.
- (36) Torchia, D. A.; Szabo, A. J. *Magn. Reson.* **1982**, 49, 107.
- (37) Bée, M. *Quasielastic Neutron Scattering*; Adam Hilger: Bristol, 1988.
- (38) Jobic, H.; Bée, M.; Kearley, J. *Zeolites* **1989**, 9, 312.
- (39) Jobic, H.; Bée, M.; Kearley, G. J. *Zeolites* **1992**, 12, 146.
- (40) Jobic, H.; Bée, M.; Caro, J. *Proceedings 9th International Zeolite Conference, Montreal, 1992*; von Ballmoos, R., Higgins, J. B., Treacy, M. M. J., Eds.; Butterworth-Heinemann: Boston, 1993; Vol. II, p 121.
- (41) Keniry, M. A.; Kintanar, A.; Smith, R. L.; Gutowsky, H. S.; Oldfield, E. *Biochemistry* **1984**, 23, 288. Kintanar, A.; Alam, T. M.; Huang, W. Ch.; Schindele, D. C.; Wemmer, D. E.; Drobny, G. *J. Am. Chem. Soc.* **1988**, 110, 6367.
- (42) Herzberg, G. *Infrared and Raman Spectra*; Van Nostrand: New York, 1945.
- (43) Demontis, P.; Suffritti, G. B. *Chem. Rev.* **1997**, 97, 2845.
- (44) A detailed analysis of the QENS data will be reported elsewhere: Jobic, H.; Bée, M. Manuscript in preparation.
- (45) Fyfe, C. A.; Strobl, H.; Kokotailo, G. T.; Kennedy, G. J.; Barlow, G. E. *J. Am. Chem. Soc.* **1988**, 110, 3373.
- (46) van Koningsveld, H.; Jansen, J. C.; van Bekkum, H. *Zeolites* **1990**, 10, 235.
- (47) Conner, W. C. Physical Adsorption in Microporous Solids. In *Physical Adsorption: Experiment, Theory and Applications*; Fraissard, J., Conner, C. W., Eds.; NATO ASI Series C: Mathematical and Physical Sciences; Kluwer Academic Publishers: Dordrecht, Boston, London, 1997; Vol. 491.
- (48) Müller, J. A.; Conner, W. C. *J. Phys. Chem.* **1993**, 97, 1451.
- (49) Lermer, H.; Draeger, M.; Steffen, J.; Unger, K. K. *Zeolites* **1985**, 5, 131.
- (50) Hernández, E.; Catlow, C. R. A. *Proc. R. Soc. London A* **1995**, 448, 143.
- (51) Flanigen, E. M.; Bennett, J. M.; Grose, R. W.; Cohen, J. P.; Patton, R. L.; Kirchner, R. M.; Smith, J. V. *Nature (London)* **1978**, 271, 512.